Angiomotin-like Proteins Associate with and Negatively Regulate YAP1*⑤

Wenqi Wang[‡], **Jun Huang**[§1], and **Junjie Chen**[‡2]

From the [‡]*Department of Experimental Radiation Oncology, The University of Texas M.D. Anderson Cancer Center, Houston, Texas 77030 and the* [§]*Life Sciences Institute, Zhejiang University, Hangzhou, Zhejiang 310058, China*

In both *Drosophila* and mammalian systems, the Hippo pathway plays an important role in controlling organ size, mainly through its ability to regulate cell proliferation and apoptosis. The key component in the Hippo pathway is the Yes-associated protein YAP1, which localizes in nucleus, functions as a transcriptional coactivator, and regulates the expression of several proliferation- and apoptosis-related genes. The Hippo pathway negatively regulates YAP1 transcriptional activity by modulating its nuclear-cytoplasmic localization in a phosphorylation-dependent manner. Here, we describe the identification of several new PY motif-containing proteins, including angiomotin-like protein 1 (AMOTL1) and 2 (AMOTL2), as YAP1-associated proteins. We demonstrate that AMOTL1 and AMOTL2 can regulate YAP1 cytoplasm-to-nucleus translocation through direct protein-protein interaction, which can occur independent of YAP1 phosphorylation status. Moreover, down-regulation of AMOTL2 in MCF10A cells promotes epithelial-mesenchymal transition, a phenotype that is also observed in MCF10A cells with YAP1 overexpression. Together, these data support a new mechanism for YAP1 regulation, which is mediated via its direct interactions with angiomotin-like proteins.

The control of organ (or organism) size is a fundamental question that has not been fully understood. The Hippo pathway has been identified as one of the pathways that control cell proliferation and apoptosis, both of which are essential for tissue and organ growth (1, 2). In *Drosophila*, core components of the Hippo pathway include two serine kinase proteins (Hippo and Warts) (3, 4), the mediator proteins (Fat, Expanded, and Merlin) (5–9), and the scaffold proteins (Mats and Salvador) (10, 11). Oncogene Yorkie has been identified as the main downstream target of the Hippo pathway (12). Yorkie is a transcriptional co-activator, which can bind transcription factor Sd (13) to enhance the expression of several proliferation and anti-apoptosis-related genes, including *cycE*, *diap1*, and *bantam* microRNA (11, 12, 14, 15) and therefore regulate growth and apoptosis.

The Hippo pathway is evolutionarily conserved. Mammalian orthologues of the components in the *Drosophila* Hippo pathway have been identified and found to be similarly important for cell proliferation and apoptosis (16). In mammalian cells, MST1/2 (Hippo orthologues) can be activated by several membrane receptors and subsequently phosphorylate downstream kinases LATS1/2 (Warts orthologues) in events that are coordinated by scaffold proteins MOB1 (Mats orthologue) and WW45 (Salvador orthologue) (16, 17). Activated LATS1/2 can directly phosphorylate YAP1 (Yorkie orthologue) at Ser[127], which provides a docking site for 14-3-3 protein and then leads to YAP1 cytoplasmic retention (18). Phosphorylated YAP1 also recruits Skp1/Cul1/F-box protein (SCF)-β-transducing repeat containing protein (β-TRCP) E3 ligase which promotes YAP1 ubiquitination and degradation in the cytoplasm (19). When YAP1 is in the nucleus, YAP1 binds to transcription factors such as TEA domain transcription factor (TEAD) and activates the transcription of proliferation and/or survival-related genes (20). Therefore, the Hippo pathway mainly regulates YAP1 via YAP1 phosphorylation at the Ser[127] site, which prevents YAP1 nuclear translocation and thus inhibits YAP1 function as a transcriptional co-activator. The translocation of YAP1 between cytoplasm and nucleus is very important for the control of cell proliferation and organ size (16, 17). Moreover, dysregulation of YAP1 greatly enhances tumorigenesis because YAP1 not only promotes cell proliferation but also leads to epithelial-mesenchymal transition (EMT),[3] which lessens cell contact inhibition and thus allows tumorigenesis (18, 21).

Although YAP1 phosphorylation represents a major route for YAP1 regulation, a recent study suggested that YAP may also be repressed in a phosphorylation-independent manner in *Drosophila* (22). In this case, the Hippo pathway components Expanded, Hippo, and Warts can directly bind to YAP1 through physical interaction between their corresponding PY motifs and the WW domains of YAP1. Thus, the regulation of YAP1 *in vivo* may be complex and warrant further investigation.

[3] The abbreviations used are: EMT, epithelial-mesenchymal transition; AMOTL, angiomotin-like protein; YAP, Yes-associated protein; SFB, S-FLAG-SBP; SBP, streptavidin binding peptide; TRITC, tetramethylrhodamine isothiocyanate.

Here, we report the identification of angiomotin (AMOT) and angiomotin-like proteins as new YAP1-associated proteins. AMOT is a vascular angiogenesis-related protein, which was initially identified as an angiogenesis inhibitor angiostatin-binding protein through a yeast two-hybrid screen (23, 24). AMOT can induce endothelial cell migration and tubule formation, and therefore, it promotes angiogenesis (23, 25). There are two other angiomotin-like proteins, AMOTL1 and AMOTL2. These three proteins belong to a new protein family with a highly conserved coil-coil domain, PDZ binding domain, and glutamine-rich domain (24). Just like AMOT, AMOTL1 and AMOTL2 also play important roles in cell migration and angiogenesis (26, 27), suggesting that this family of proteins may share similar functions *in vivo*.

In this study, we demonstrate that AMOT, AMOTL1, and AMOTL2 specifically interact with YAP1. This interaction is important for the regulation of YAP1 cytoplasm-to-nucleus translocation. Just like YAP1 overexpression, down-regulation of AMOTL2 in MCF10A cells promotes EMT. Together, these data suggest that YAP1 is regulated *in vivo* via its direct interactions with angiomotin-like proteins.

EXPERIMENTAL PROCEDURES

Antibodies—Anti-AMOTL1, FLAG, HA, α-tubulin, and β-actin were obtained from Sigma. Anti-phospho-YAP1 (Ser[127]), AKT, phospho-AKT, ERK, and phospho-ERK were purchased from Cell Signaling Technology. Anti-YAP1, Myc and GFP were obtained from Santa Cruz Biotechnology. The AMOT polyclonal antibody was raised against a glutathione *S*-transferase (GST)-AMOT (1–675 amino acids) fusion protein. AMOTL2 polyclonal antibody was raised against a Maltose binding protein (MBP)-AMOTL2 (501–780 amino acids) fusion protein. Anti-YAP1 serum was raised against GST-YAP1 full-length fusion protein. Antisera were affinity-purified using the AminoLink Plus immobilization and purification kit (Pierce).

Plasmids—All constructs were generated by PCR and subcloned into pDONOR201 vector using Gateway technology (Invitrogen). The entry clones were transferred subsequently into Gateway-compatible destination vectors.

PCR-mediated site-directed mutagenesis was used to generate point mutations or deletions. All these constructs include YAP1 Ser[127] to Ala mutation, YAP1 WW domain deletions (deletion of the first WW domain, WW1D, missing residues 172–203 or deletion of the second WW domain, WW2D, missing residues 232–263), and WW domain mutations (WW1m contains Trp[199] to Ala and Pro[202] to Ala mutations, WW2m contains Trp[258] to Ala and Pro[261] to Ala mutations) were verified by sequencing. Plasmids encoding FLAG-tagged wild-type AMOTL1 and two PY motif mutated constructs were kindly provided by Professor Anthony P. Schmitt (Pennsylvania State University). Plasmid encoding AMOTL2 was kindly provided by Professor Anming Meng (Tsinghua University), and the mutation of its PY motif (Tyr[213] to Ala) was created through PCR-mediated site-directed mutagenesis.

Cell Culture and Transfection—HeLa and 293T cells were purchased from ATCC (Manassas, VA) and maintained in DMEM medium supplemented with 10% FBS at 37 °C in 5% CO_2 (v/v). MCF10A cells were kindly provided from Professor Dihua Yu (M.D. Anderson Cancer Center). MCF10A cells were maintained in DMEM/F12 medium supplemented with 5% horse serum, 200 ng/ml EGF, 500 ng/ml hydrocortisone, 100 ng/ml cholera toxin, and 10 μg/ml insulin at 37 °C in 5% CO_2 (v/v). Cell transfection was performed using Lipofectamine 2000 (Invitrogen) following the protocol provided by the manufacturer or polyethyleneimine (Sigma).

Establishment of Stable Cell Lines and Affinity Purification of S-FLAG-SBP (SFB)-tagged Protein Complexes—293T cells were transfected with plasmids encoding various SFB-tagged proteins. Stable cell lines were selected by 2 μg/ml puromycin and confirmed by immunostaining and Western blotting. MCF10A cells were infected by lentivirus expressing Tet-On inducible SFB-tagged proteins, and stable pools were selected by 500 μg/ml G418 and confirmed by immunostaining and Western blotting.

For affinity purification, 293T or MCF10A cells were lysed in NETN buffer (20 mM Tris-HCl, pH 8.0, 100 mM NaCl, 1 mM EDTA, 0.5% Nonidet P-40) (with protease inhibitors) at 4 °C for 20 min. Crude lysates were centrifuged at 4 °C, 14,000 rpm for 15 min. Supernatants were incubated with streptavidin-conjugated beads (Amersham Biosciences) for 2 h at 4 °C. Beads were washed three times with NETN buffer, and bounded proteins were eluted with NETN buffer containing 2 mg/ml biotin (Sigma). Elutes were incubated with S protein beads (Novagen). Beads were washed three times with NETN buffer, and protein mixtures were subjected to mass spectrometry analysis.

GST Pulldown Assay—GST fusion proteins were expressed and purified from *Escherichia coli* BL21 cells. 2 μg of GST fusion proteins were immobilized on glutathione-Sepharose 4B beads and incubated with various cell lysates for 2 h at 4 °C. Beads were washed three times. Proteins bound to beads were eluted and subjected to SDS-PAGE and Western blotting analysis.

Immunofluorescent Staining—Cells cultured on coverslips were fixed by 4% paraformaldehyde for 10 min at room temperature and then extracted with 0.5% Triton X-100 solution for 5 min. After being blocked with 1% BSA, cells were incubated with the indicated primary antibodies for 1 h at room temperature. After that, cells were washed and incubated with FITC or rhodamine-conjugated secondary antibodies for 1 h. Cells were counterstained with 1 ng/ml DAPI for 2 min for the visualization of nuclear DNA.

Lentivirus Packaging and Infection—Inducible lentiviral vector and packaging plasmids (pMD2G and pSPAX2) were kindly provided by Professor Songyang Zhou (Baylor College of Medicine). Briefly, lentiviral plasmids encoding the indicated proteins were cloned into SFB-tagged lentiviral vector using Gateway technology. MCF10A cells were infected with viral supernatants with the addition of 8 μg/ml Polybrene, and stable pools were selected with medium containing 500 μg/ml G418. The expression of the indicated genes in the sta-

A

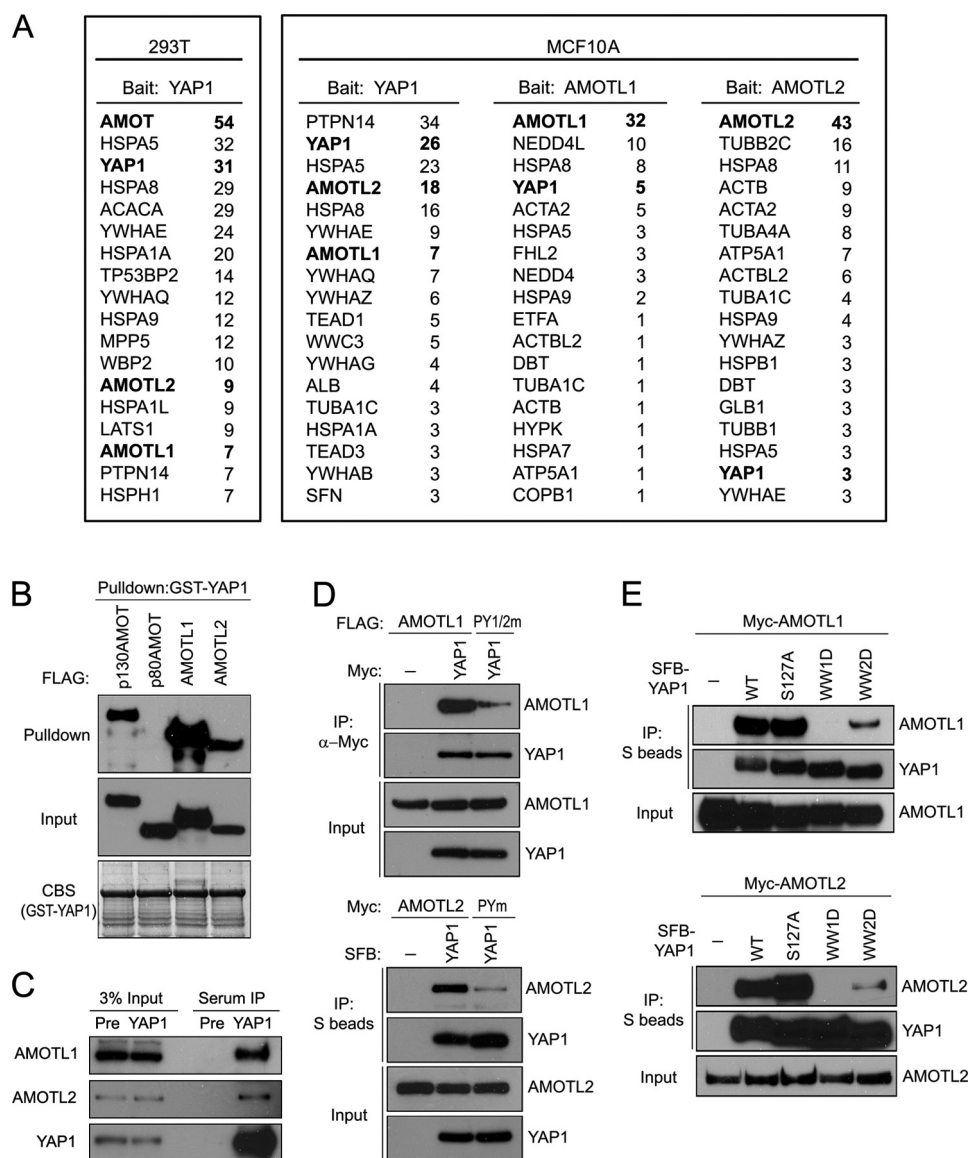| 293T		MCF10A					
Bait: YAP1		**Bait: YAP1**		**Bait: AMOTL1**		**Bait: AMOTL2**	
AMOT	**54**	PTPN14	34	**AMOTL1**	**32**	**AMOTL2**	**43**
HSPA5	32	**YAP1**	**26**	NEDD4L	10	TUBB2C	16
YAP1	**31**	HSPA5	23	HSPA8	8	HSPA8	11
HSPA8	29	**AMOTL2**	**18**	**YAP1**	**5**	ACTB	9
ACACA	29	HSPA8	16	ACTA2	5	ACTA2	9
YWHAE	24	YWHAE	9	HSPA5	3	TUBA4A	8
HSPA1A	20	**AMOTL1**	**7**	FHL2	3	ATP5A1	7
TP53BP2	14	YWHAQ	7	NEDD4	3	ACTBL2	6
YWHAQ	12	YWHAZ	6	HSPA9	2	TUBA1C	4
HSPA9	12	TEAD1	5	ETFA	1	HSPA9	4
MPP5	12	WWC3	5	ACTBL2	1	YWHAZ	3
WBP2	10	YWHAG	4	DBT	1	HSPB1	3
AMOTL2	**9**	ALB	4	TUBA1C	1	DBT	3
HSPA1L	9	TUBA1C	3	ACTB	1	GLB1	3
LATS1	9	HSPA1A	3	HYPK	1	TUBB1	3
AMOTL1	**7**	TEAD3	3	HSPA7	1	HSPA5	3
PTPN14	7	YWHAB	3	ATP5A1	1	**YAP1**	**3**
HSPH1	7	SFN	3	COPB1	1	YWHAE	3

FIGURE 1. **Identification of AMOTL1 and AMOTL2 proteins as YAP1associated proteins in MCF10A cells.** *A*, mass spectrometry analysis revealed YAP1-associated proteins identified in 293T and MCF10A cells. AMOTL1- and AMOTL2-associated proteins were also revealed by mass spectrometry analysis in MCF10A cells. The number of peptides for each protein identified by mass spectrometry analysis was listed. *B*, GST-YAP1 fusion proteins immobilized on Sepharose beads were incubated with cell lysates containing exogenously expressed SFB-tagged p130AMOT, p80AMOT (negative control), AMOTL1, or AMOTL2. Immunoblotting was conducted using antibodies as indicated. *CBS*, Coomassie Blue staining. *C*, immunoprecipitation (*IP*) was conducted using anti-YAP1 serum or prebleed serum and lysates prepared from 293T cells. Associated endogenous AMOTL1 and AMOTL2 were revealed by immunoblotting with anti-AMOTL1 and anti-AMOTL2 antibodies, respectively. *Pre*, prebleed serum control. *D*, Myc-tagged or SFB-tagged YAP1 was used to precipitate wild-type AMOTL1/AMOTL2 or two PY motifs mutated AMOTL1 (*PY1/2m*)/PY motif mutated AMOTL2 (*PYm*) (see "Experimental Procedures"). Immunoblotting was conducted using the indicated antibodies. *E*, S protein beads were used to pull down SFB-tagged wild-type, S127A mutant, or WW domain mutant YAP1 (see "Experimental Procedures") from lysates containing exogenously expressed Myc-AMOTL1 or Myc-AMOTL2. Immunoblotting was conducted using antibodies as indicated.

ble pools was induced by the addition of 1 μg/ml doxycycline for 36 h for the experiments presented in this report.

AMOT (used as control), AMOTL1, AMOTL2, and YAP1 shRNA sets were all purchased from Open Biosystems. The target sequence for AMOT was: 5′-ggcctgtgttccactccaat-3′; for AMOTL1, 5′-ccatgagaaacaaattggaa-3′; for AMOTL2, 5′-cagtaccctcatgttgtacta-3′; and for YAP1, 5′-caggtgatactatc-aaccaaa-3′.

Wound Healing Assay—Confluent cells were scratched with 1-ml pipette tips, washed twice with PBS, and then incubated with the appropriate medium. 22 h later, images were captured under a microscope.

RESULTS

Identification of AMOT, AMOTL1, and AMOTL2 Proteins as YAP1-associated Proteins—To identify YAP1-associated proteins, we established 293T cells stably expressing full-length YAP1 fused with an N-terminal S epitope-FLAG-SBP (streptavidin binding peptide) tag (SFB-YAP1). We performed tandem affinity purification and identified AMOT as the major YAP1-associated protein (Fig. 1*A*). To elucidate the cellular function of AMOT protein, we compared different cell lines and found that the AMOT protein level is very low in many other cell lines (such as MCF10A, HeLa, NIH3T3, and

Madin-Darby canine kidney cells) as compared with that observed in 293T cells (data not shown). We speculated that other proteins might substitute for AMOT function in these cell lines. Thus, we generated an MCF10A derivative cell line stably expressing SFB-tagged YAP1. Interestingly, we identified two other AMOT family proteins, angiomotin-like protein 1 (AMOTL1) and angiomotin-like protein 2 (AMOTL2), in this purification (Fig. 1*A*). As a matter of fact, these two proteins were also identified as YAP1-associated proteins when we performed purification in 293T cells (Fig. 1*A*). Moreover, when we conducted reverse tandem affinity purification in MCF10A cells using SFB-tagged AMOTL1 or AMOTL2, we also uncovered YAP1 as AMOTL1- or AMOTL2-associated protein (Fig. 1*A*). Together, these data indicate that AMOTL1 and AMOTL2 probably associate with YAP1 and may regulate YAP1 function in MCF10A cells.

Consistent with our purification results, both AMOTL1 and AMOTL2 interacted with YAP1, and the association between AMOTL1 or AMOTL2 with YAP1 was as strong as the AMOT/YAP1 interaction (Fig. 1*B*; please also see supplemental Fig. 1). Co-immunoprecipitation experiments further confirmed endogenous interactions between YAP1 and AMOTL1 or AMOTL2 (Fig. 1*C*).

The interaction of AMOTL1 or AMOTL2 with YAP1 was independent of YAP1 phosphorylation at the Ser[127] site (Fig. 1*E*). These interactions were mainly mediated by the first WW domain of YAP1, whereas the deletion of the second WW domain also decreased the interactions between YAP1 and AMOTL1 or AMOTL2 (Fig. 1*E*).

Because mutations in YAP1 WW domains could abolish or decrease its interaction with AMOTL1 or AMOTL2, we speculated that these interactions might be mediated by the PY motifs in these AMOT-like proteins. There are two PY motifs in AMOTL1 ([309]PPPEY[313], [366]PPPEY[370]) and one PY motif in AMOTL2 ([209]PPPQY[213]). Mutating these PY motifs in either AMOTL1 or AMOTL2 dramatically decreased their interactions with YAP1 (Fig. 1*D*). Taken together, these results suggest that the interaction of AMOTL1 or AMOTL2 with YAP1 is mediated by the WW domains of YAP1 and the PY motifs in AMOTL1 or AMOL2.

AMOTL1 and AMOTL2 Regulate YAP1 Cytoplasm-to-Nucleus Translocation—Because AMOTL1 and AMOTL2 are cytoplasmic proteins, whereas YAP1 can shuttle between nucleus and cytoplasm, we next tested whether AMOTL1 and AMOTL2 could regulate YAP1 subcellular localization. Indeed, AMOTL1 or AMOTL2 expression resulted in the localization of endogenous YAP1- or SFB-tagged YAP1 to cytoplasm in HeLa cells (Fig. 2, *A* and *B*). Moreover, this AMOTL1- or AMOTL2-dependent cytoplasmic localization of YAP1 was blocked when we used a YAP1 mutant with deletion of its first WW domain (Fig. 2*C*). On the other hand, when the YAP1 Ser[127] phosphorylation site was mutated to Ala, AMOTL1 or AMOTL2 was still able to promote the cytoplasmic localization of this S127A mutant of YAP1 (Fig. 2*D*). These data suggest that AMOTL1 and AMOTL2 can regulate subcellular localization of YAP1, which is mediated by direct protein-protein interaction and does not require YAP1 phosphorylation at Ser[127] site.

AMOTL2 Down-regulation Leads to EMT in MCF10A Cells—Earlier studies demonstrated that YAP1 overexpression leads to EMT in MCF10A cells (21). Because AMOTL1 and AMOTL2 can retain YAP1 in cytosol and thus inhibit YAP1 function in the nucleus, we wondered whether down-regulation of AMOTL1 or AMOTL2 would lead to EMT in MCF10A cells.

We used lentiviral shRNAs, which efficiently targeted the down-regulation of AMOTL1 and AMOTL2 (Fig. 3*A*). RT-PCR confirmed that endogenous transcripts of AMOTL1 or AMOTL2 were respectively decreased in these stable pools (Fig. 3*B*). Although we could not detect the expression of AMOTL1 in MCF10A cells by Western blotting (data not shown), we were able to detect endogenous AMOTL2 (Fig. 3*C*) and confirmed the down-regulation of endogenous AMOTL2 protein level in these knockdown cells (Fig. 3*C*).

We noticed that cell morphology was dramatically altered in AMOTL2 stable knockdown cells, which look like spindle-shaped fibroblast cells, whereas AMOTL1 stable knockdown cells maintained epithelial morphology (Fig. 3*D*). In AMOTL2 knockdown cells, the expression of epithelial marker E-cadherin decreased and the expression of mesenchymal markers N-cadherin and vimentin increased, whereas there was no change of the expression of these markers in AMOTL1 knockdown cells (Fig. 3*E*). AMOTL2 knockdown cells also showed reduced cell-cell junction when they grew confluent, whereas AMOTL1 knockdown cells kept intact cell-cell junction (Fig. 3*F*). Moreover, AMOTL2 knockdown cells migrate faster than control MCF10A cells or AMOTL1 knockdown cells (Fig. 3*G*). All of these indicate that AMOTL2 knockdown leads to EMT in MCF10A cells.

Specifically, the EMT phenotypes observed in AMOTL2 knockdown cells were partially reversed when YAP1 expression was down-regulated at the same time (Fig. 3*H*), indicating that YAP1 is at least one of the downstream targets of AMOTL2 in this process. In addition, the nucleus-to-cytoplasm translocation of YAP1 in confluent cells was reduced (Fig. 3*I*), and YAP1 phosphorylation also decreased in AMOTL2 knockdown cells (Fig. 3*J*). Moreover, the AKT and ERK pathways were also activated in AMOTL2 knockdown cells (Fig. 3*J*), which is similar to what has been reported in cells with YAP1 overexpression (21). Together, these data suggest that down-regulation of AMOTL2 results in enhanced nuclear localization of YAP1 and EMT in MCF10A cells.

DISCUSSION

Here, we reported the identification of several new YAP1-associated proteins, AMOT, AMOTL1, and AMOTL2. Their interactions with YAP1 are mediated by the PY motifs in AMOT-like proteins and WW domains in the central region of YAP1. Moreover, these direct protein-protein interactions are involved in the regulation of YAP1 localization and function *in vivo*. These results indicate that AMOT-like proteins belong to a new group of YAP1 regulators that may play important roles in controlling cell proliferation and contact-contact inhibition.
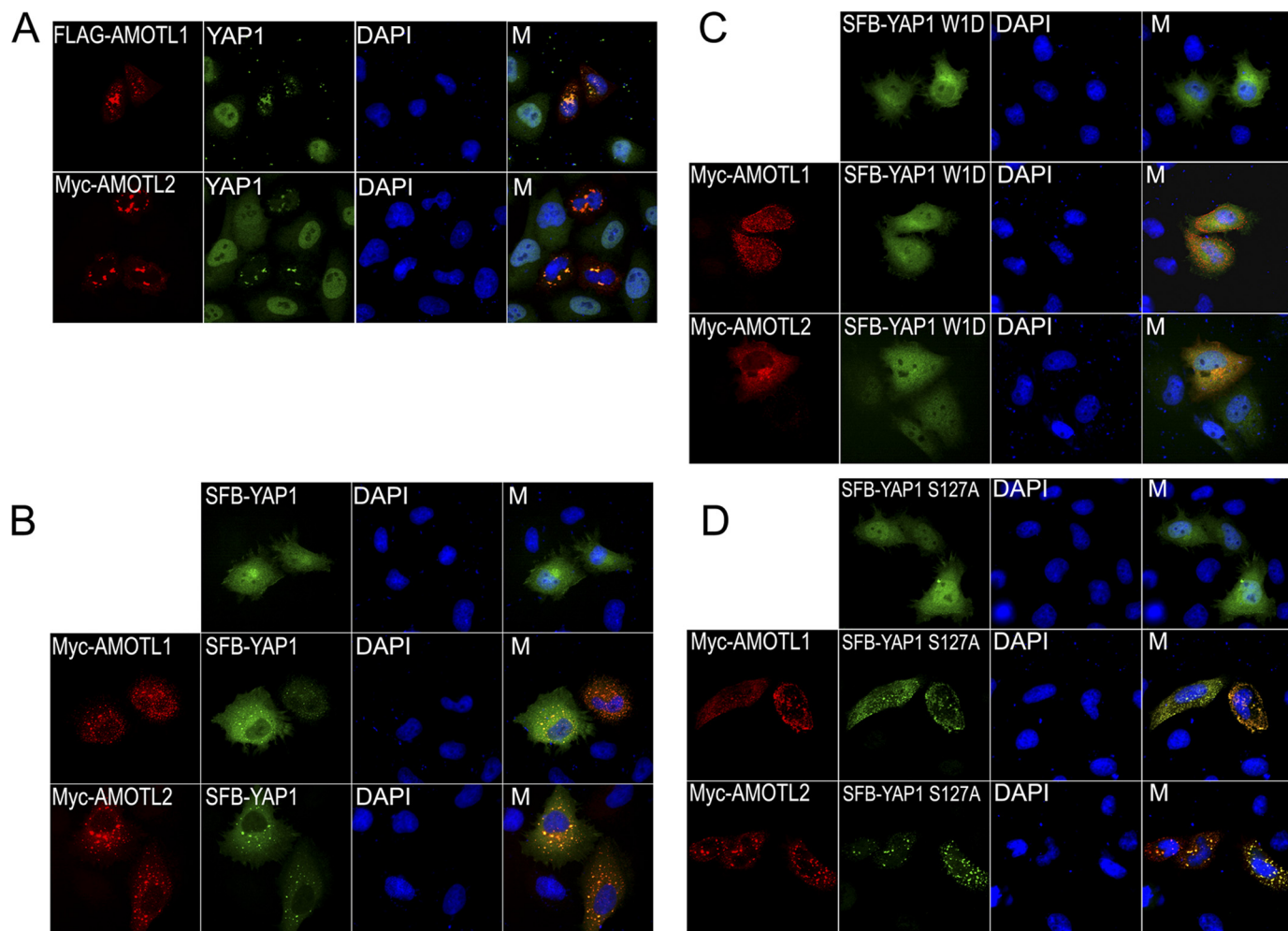
FIGURE 2. **AMOTL1 and AMOTL2 regulate YAP1 subcellular localization.** *A*, the localization of endogenous YAP1 was revealed by anti-YAP1 immunostaining in cells with or without AMOTL1 or AMOTL2 overexpression. *B–D*, HeLa cells were transfected with plasmids encoding Myc-tagged AMOTL1 or AMOTL2 with plasmids encoding SFB-tagged wild-type YAP1 (*B*), YAP1 mutant with deletion of its first WW domain (*C*), or YAP1 S127A mutant (*D*). Immunostaining was conducted using antibodies as indicated. *M*, merged.

The major regulation of YAP1 activity appears to be at its subcellular localization. The activation of the Hippo pathway leads to YAP1 phosphorylation, which promotes its cytoplasmic localization via the binding of phosphorylated YAP1 to 14-3-3 proteins in the cytosol and thus inhibits the transactivation activity of YAP1 *in vivo*. In this study, we showed that AMOT-like proteins could also keep YAP1 in the cytoplasm. In this case, the maintenance of YAP1 cytoplasmic localization does not depend on its phosphorylation status. Instead, it is mediated by direct protein-protein interaction between AMOT-like proteins and YAP1.

AMOTL1 and AMOTL2 belong to a new family of proteins including AMOT. AMOTL1 shares ~60% homologous with AMOT and has an expression pattern similar to AMOT in endothelial cell (28). We showed that just like AMOTL1 and AMOTL2, AMOT also binds directly to YAP1 via the WW domain of YAP1 and the PY motifs located at the N terminus of AMOT (please see supplemental Fig. 1). Likewise, AMOT could also mediate YAP1 cytoplasmic localization (supplemental Fig. 1*G*). Thus, all three members of this protein family behave similarly because each of them can interact with YAP1 and regulate YAP1

subcellular localization. The relative importance of these three family members in various cell lines or tissues may be determined by their expression levels. For example, AMOT expression is undetectable in MCF10A cells. Although both AMOTL1 and AMOTL2 are expressed in MCF10A cells based on RT-PCR analysis (Fig. 3*B*), we were unable to detect the expression of AMOTL1 by Western blotting (data not shown), implying that the expression of AMOTL1 may be quite low in these cells. In support of this possibility, we obtained more peptides derived from AMOTL2 than those derived from AMOTL1 from YAP1 purification in MCF10A cells (Fig. 1*A*). It is likely that this difference in protein expression may explain why down-regulation of AMOTL2 alone is sufficient to lead to deregulation of YAP1 localization and promote epithelial-mesenchymal transition in MCF10A cells (Fig. 3). It remains to be determined whether the AMOT family members may have tissue-specific expression and thus play different roles in regulating YAP1 function in various tissues or organs. Of course, it is also possible that different members of this protein family may have some distinct functions, which still needs further investigation.
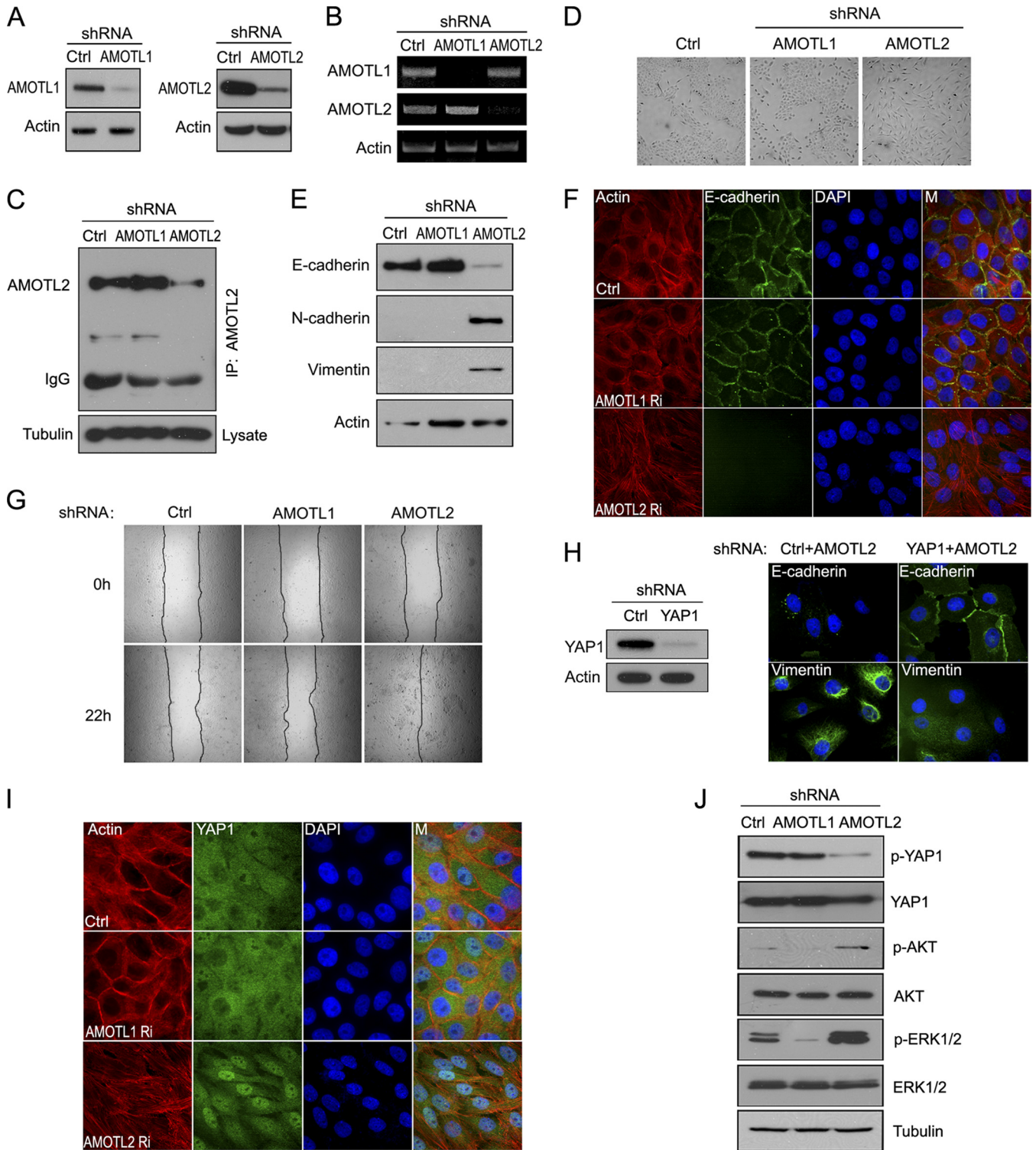
FIGURE 3. **Down-regulation of AMOTL2 causes EMT in MCF10A cells.** *A*, 293T cells were transfected with the indicated shRNAs together with plasmids encoding FLAG-tagged AMOTL1 or AMOTL2. Cells were collected 72 h later and subjected to Western blotting. *Ctrl*, control. *B*, the level of AMOTL1 or AMOTL2 transcripts was revealed by RT-PCR in the indicated stable knockdown cells. *C*, immunoprecipitation (*IP*) and immunoblotting were performed using anti-AMOTL2 serum and cell lysates prepared from the indicated cell lines. For each immunoprecipitation, a total of 1 mg of the indicated protein lysates was used. Anti-tubulin immunoblotting was included as a control. *D*, lentiviral shRNAs were used to infect MCF10A cells, and stable knockdown pools were generated. Bright field pictures were captured to reveal cell morphology in these pools. *E*, cells with AMOTL2 down-regulation displayed EMT phenotypes. E-cadherin was used as epithelial marker. N-cadherin and vimentin were used as mesenchymal markers. *F*, cell-cell junction was diminished in AMOTL2 knockdown cells. E-cadherin was used as cell-cell junction marker. Actin filaments were labeled by TRITC-phalloidin. *M*, merged. *G*, cell migration capability increased in AMOTL2 knockdown cells as determined by wound healing assay. *H*, MCF10A cells were infected with the indicated lentiviral shRNAs respectively, and stable pools were used for immunostaining with anti-E-cadherin and anti-vimentin antibodies. The efficiency of YAP1 down-regulation by shRNAs was verified by anti-YAP1 immunoblotting. *I*, YAP1 retained its dominant nuclear localization in AMOTL2 knockdown (*Ri*) cells even when cells reached confluence. *M*, merged. *J*, YAP1 phosphorylation (*p-YAP1*) decreased in AMOTL2 knockdown MCF10A cells. AKT and ERK signaling pathways were also activated in AMOTL2 knockdown cells. *p-AKT*, AKT phosphorylation; *p-ERK1/2*, ERK1/2 phosphorylation.

Angiomotin-like Proteins Negatively Regulate YAP1

REFERENCES

1. Harvey, K., and Tapon, N. (2007) *Nat. Rev. Cancer* **7,** 182–191
2. Pan, D. (2007) *Genes Dev.* **21,** 886–897
3. Harvey, K. F., Pfleger, C. M., and Hariharan, I. K. (2003) *Cell* **114,** 457–467
4. Dan, I., Watanabe, N. M., and Kusumi, A. (2001) *Trends Cell Biol.* **11,** 220–230
5. Cho, E., Feng, Y., Rauskolb, C., Maitra, S., Fehon, R., and Irvine, K. D. (2006) *Nat. Genet.* **38,** 1142–1150
6. Bennett, F. C., and Harvey, K. F. (2006) *Curr. Biol.* **16,** 2101–2110
7. Hamaratoglu, F., Willecke, M., Kango-Singh, M., Nolo, R., Hyun, E., Tao, C., Jafar-Nejad, H., and Halder, G. (2006) *Nat. Cell Biol.* **8,** 27–36
8. McClatchey, A. I., and Giovannini, M. (2005) *Genes Dev.* **19,** 2265–2277
9. Okada, T., You, L., and Giancotti, F. G. (2007) *Trends Cell Biol.* **17,** 222–229
10. Lai, Z. C., Wei, X., Shimizu, T., Ramos, E., Rohrbaugh, M., Nikolaidis, N., Ho, L. L., and Li, Y. (2005) *Cell* **120,** 675–685
11. Tapon, N., Harvey, K. F., Bell, D. W., Wahrer, D. C., Schiripo, T. A., Haber, D. A., and Hariharan, I. K. (2002) *Cell* **110,** 467–478
12. Huang, J., Wu, S., Barrera, J., Matthews, K., and Pan, D. (2005) *Cell* **122,** 421–434
13. Goulev, Y., Fauny, J. D., Gonzalez-Marti, B., Flagiello, D., Silber, J., and Zider, A. (2008) *Curr. Biol.* **18,** 435–441
14. Nolo, R., Morrison, C. M., Tao, C., Zhang, X., and Halder, G. (2006) *Curr. Biol.* **16,** 1895–1904
15. Thompson, B. J., and Cohen, S. M. (2006) *Cell* **126,** 767–774
16. Zeng, Q., and Hong, W. (2008) *Cancer Cell* **13,** 188–192
17. Zhao, B., Lei, Q. Y., and Guan, K. L. (2008) *Curr. Opin. Cell Biol.* **20,** 638–646
18. Zhao, B., Wei, X., Li, W., Udan, R. S., Yang, Q., Kim, J., Xie, J., Ikenoue, T., Yu, J., Li, L., Zheng, P., Ye, K., Chinnaiyan, A., Halder, G., Lai, Z. C., and Guan, K. L. (2007) *Genes Dev.* **21,** 2747–2761
19. Zhao, B., Li, L., Tumaneng, K., Wang, C. Y., and Guan, K. L. (2010) *Genes Dev.* **24,** 72–85
20. Zhao, B., Ye, X., Yu, J., Li, L., Li, W., Li, S., Yu, J., Lin, J. D., Wang, C. Y., Chinnaiyan, A. M., Lai, Z. C., and Guan, K. L. (2008) *Genes Dev.* **22,** 1962–1971
21. Overholtzer, M., Zhang, J., Smolen, G. A., Muir, B., Li, W., Sgroi, D. C., Deng, C. X., Brugge, J. S., and Haber, D. A. (2006) *Proc. Natl. Acad. Sci. U.S.A.* **103,** 12405–12410
22. Ren, F., Zhang, L., and Jiang, J. (2010) *Dev. Biol.* **337,** 303–312
23. Troyanovsky, B., Levchenko, T., Månsson, G., Matvijenko, O., and Holmgren, L. (2001) *J. Cell Biol.* **152,** 1247–1254
24. Bratt, A., Wilson, W. J., Troyanovsky, B., Aase, K., Kessler, R., Van Meir, E. G., and Holmgren, L. (2002) *Gene* **298,** 69–77
25. Bratt, A., Birot, O., Sinha, I., Veitonmäki, N., Aase, K., Ernkvist, M., and Holmgren, L. (2005) *J. Biol. Chem.* **280,** 34859–34869
26. Gagné, V., Moreau, J., Plourde, M., Lapointe, M., Lord, M., Gagnon, E., and Fernandes, M. J. (2009) *Cell Motil. Cytoskeleton* **66,** 754–768
27. Huang, H., Lu, F. I., Jia, S., Meng, S., Cao, Y., Wang, Y., Ma, W., Yin, K., Wen, Z., Peng, J., Thisse, C., Thisse, B., and Meng, A. (2007) *Development* **134,** 979–988
28. Zheng, Y., Vertuani, S., Nyström, S., Audebert, S., Meijer, I., Tegnebratt, T., Borg, J. P., Uhlén, P., Majumdar, A., and Holmgren, L. (2009) *Circulation Res.* **105,** 260–270